Evidence of ^{4}He Crystallization via Quantum Tunneling at mK Temperatures

J. P. Ruutu, P. J. Hakonen, J. S. Penttilä, A. V. Babkin, J. P. Saramäki, and E. B. Sonin*

Low Temperature Laboratory, Helsinki University of Technology, Otakaari 3A, FIN-02150 Espoo, Finland

(Received 29 April 1996)

We have investigated creation of ^{4}He crystals from the superfluid phase at the temperature range 2 mK–1.0 K. Statistical nucleation-event distributions in overpressure were found to be broad, asymmetric, and temperature independent below 100 mK. Our statistical analysis agrees with a theoretical model suggesting that solid formation is driven by macroscopical quantum-mechanical fluctuations from a seed preexisting in a cavity on the wall. [S0031-9007(96)00821-6]

PACS numbers: 67.80.–s, 64.70.Dv

The phenomenon of macroscopic quantum tunneling (MQT) has attracted attention of experimentalists and theorists for many years [1,2]. The most extraordinary feature of it is that a macroscopic object with many degrees of freedom manifests nonclassical behavior calculable only using quantum mechanics. MQT has been observed to play a role in a number of physical processes, e.g., in superfluids [3–6] and in superconductors [7]. Perhaps the most detailed experimental and theoretical analysis has been performed for the escape rate from the zero-voltage state of small Josephson junctions [2,8]. In addition to observation of temperature-independent escape rate, which is the first sign of quantum tunneling, statistical analysis indicated a good agreement between theory and experiment. However, contrary to the usual microscopic quantum tunneling, dissipation processes were significant in these experiments, which may shadow the pure quantum mechanical nature of the phenomenon.

Owing to the large mobility of the superfluid/solid interface, crystallization of solid ^{4}He is not limited by dissipation processes and, therefore, ^{4}He provides a good model for studies of MQT. In this Letter we report the first detailed study on the formation of solid from the superfluid phase of ^{4}He at low temperatures. As in the previous measurements [9] where a tendency to temperature-independent nucleation below 0.5 K was observed, solid formation in our experiments takes place at pressures much below the values of quantum nucleation predicted for bulk solidification by Lifshitz and Kagan [1], i.e., the nucleation takes place at surfaces. We have performed extensive statistical analysis on the nucleation pressures which, below 100 mK, yields a temperature-independent crystal-formation rate, growing exponentially with overpressure as is characteristic to quantum-tunneling processes. Comparison with theoretical results, based on a simple generic "quadratic + cubic" potential [2], leads to the conclusion that our results support the idea of solid formation by quantum tunneling from a seed which preexisted in a cavity at the walls.

Our experimental chamber was a polished copper cylinder ($\phi = 17$ mm, height $= 18$ mm). As in our previous optical experiments [10], the lower and upper ends of the cell were sealed with antireflection coated fused silica windows. The cell was connected to a copper nuclear demagnetization stage via a sintered silver heat exchanger with 100 m^2 surface area; the total liquid volume of the setup was 20 cm^3. Temperatures were measured using a Pt-wire NMR thermometer mounted on the top flange of nuclear stage ($T = 2$–70 mK) and with a carbon resistor located on the mixing chamber (20–1000 mK). The basic heat leak to the nuclear stage was about 30 nW. When pulsed illumination was used, the heat input increased by 0.02–6 nW, depending on the frequency of pulsing. Liquid pressure was determined using a Straty-Adams type capacitive gauge having a sensitivity of 6 pF/bars at the operating point. Outside the cryostat the filling capillary of the cell was connected to a 100 cm^3 ballast volume, which could be heated by an electric heater in order to control the flow to the sample cell. The ^{4}He gas used in the experiments was regular commercial gas with a nominal purity of 10^{-7}.

Figure 1 shows a typical single nucleation event as recorded on our pressure gauge. Before time t_0, the crystal on the bottom of the cell melts at a speed of $\dot{n} \approx -10$ μmol/s at the melting pressure p_0. The crystal vanishes at $t = t_0$, and at $t = t_1$ the flow to the ballast volume is stopped. This is enough to increase the pressure in the cell, since the evaporated cold gas in the filling line warms and expands. The overpressure $p - p_0$ increases owing to the feed $\dot{n} = 1$ μmol/s until the value p_2 at

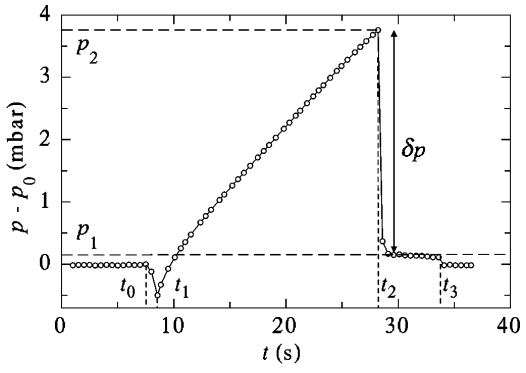

FIG. 1. Nucleation of a ^{4}He crystal. See text for details.

 0031-9007/96/77(12)/2514(4)$10.00

$t = t_2$ when the nucleation occurs, leading to an abrupt drop in pressure down to a level p_1. This jump $\delta p = p_2 - p_1 \sim 3.5$ mbar is the overpressure required for the nucleation of a new crystal; the value is close, but slightly smaller than those observed in previous experiments [9,11]. The hydrostatic pressure difference between levels p_0 and p_1 indicates that the new crystal nucleates 10 mm above the bottom of the cell. Finally, at $t = t_3$, the crystal drops to the bottom of the sample cell resulting again in the pressure p_0.

A particular nucleation site persisted in our experiments at a fixed temperature if the pressure was not decreased more than 10 mbar below the melting curve. This was confirmed by the invariance of the hydrostatic pressure difference $p_1 - p_0$ within ± 0.01 mbar. We also checked optically that the crystal entered the center of the sample cell always from the same direction. The nucleation site did change randomly when a pressure drop on the order of 0.8 bar was applied to the sample. As a function of temperature, we had a reversible change between two different nucleation sites: Above 100 mK the nucleation site switched over to a new position which then remained operational up to 1 K, returning back to the original at 100 mK upon cooling. The crossover between the low and high temperature sites was between 100 and 200 mK so that at 100 mK a small amount of events occurred at the high temperature site and vice versa at 200 mK. Starting from 50 mK downwards and from 350 mK upwards all the events came from one site.

We recorded typically 50–100 single nucleations at one temperature. When these events are ordered according to the magnitude of overpressure we obtain cumulative distributions illustrated in Fig. 2. The distributions are broad and asymmetric indicating statistical nucleation at an overpressure-dependent rate w. It should be noted that the positions of these distributions at two different temperatures are clearly separated on the overpressure axis. The widths, on the other hand, remain roughly the same at different temperatures. Thus it is reasonable to use the median values δp_m of the distributions to characterize the required overpressure for nucleation. The change in the overpressure δp_m as a function of temperature is illustrated in Fig. 3. Below 100 mK the overpressure does not depend anymore on temperature, as expected for quantum tunneling phenomena.

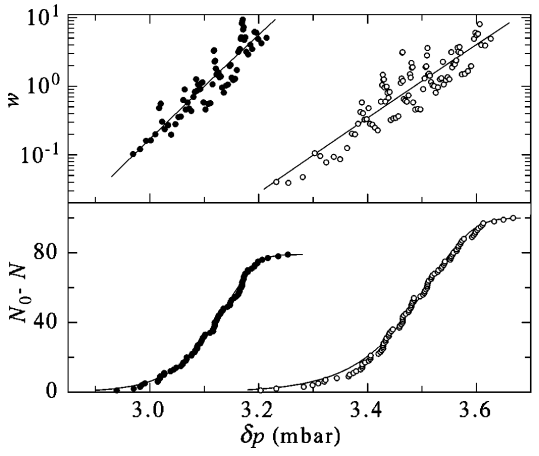

FIG. 2. Lower part shows cumulative distributions $N_0 - N$ measured at $T = 20$ mK (on the right) and at $T = 500$ mK. The upper frame illustrates the nucleation rates deduced from the cumulative distributions using Eq. (2). The solid curves at $T = 500$ mK illustrate fits obtained from Eq. (8) with $B_t = 8.3$ mbar$^{-3/2}$ and $\delta p_c = 5.1$ mbar, while the fits at 20 mK were made with Eq. (10) using $B_q = 5.8$ mbar$^{-5/4}$ and $\delta p_c = 8.0$ mbar.

The nucleation rate can be deduced from the measured cumulative distributions. Since a set of nucleation events N_0 can be considered as an ensemble of "radioactive" nuclei, the number N of events without nucleation will decay according to the standard equation

$$\frac{dN}{dt} = -w(t)N\,, \tag{1}$$

where the nucleation rate $w(t)$ is time dependent because of the variation of overpressure in time. If pressurization is linear in time, $\delta p(t) \sim ct$, we may write for the nucleation rate

$$w = c\,\frac{d}{d(\delta p)}\left[-\ln\left(\frac{N}{N_0}\right)\right]. \tag{2}$$

The use of Eq. (2) requires a numerical derivative which can be obtained reasonably well from the measured distributions after smoothing twice over five adjacent points; the upper frame of Fig. 2 illustrates the resulting nucleation rates w on logarithmic scale. The exponential nature of nucleation probabilities is evident, and an increase by a factor of $\sim$100 in the nucleation rate takes place between 3.2 and 3.6 mbar and 2.9 and 3.2 in the data at $T = 20$ and 500 mK, respectively. In order to improve statistics for a more detailed analysis, we have collected all our temperature-independent data below

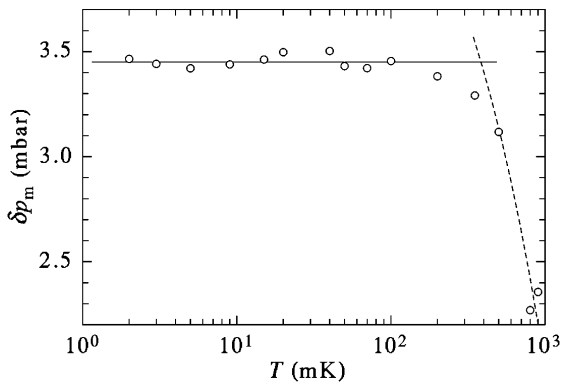

FIG. 3. Median values of the measured cumulative distributions as a function of T. The dashed curve depicts the expected temperature dependence for thermally induced nucleation [Eq. (8)]. The solid curve illustrates the average median value in the quantum regime.

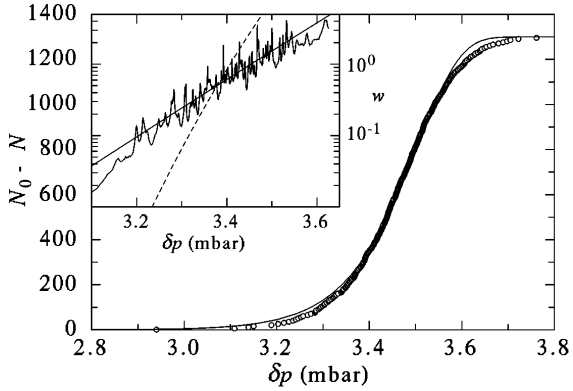

FIG. 4. Cumulative distribution of data below 100 mK measured at the average pressurization rate $\overline{c} = 0.2$ mbar/s. The inset shows the nucleation rate obtained from the data using Eq. (2). The solid curve in the inset shows a fit of Eq. (10) with $B_q = 5.1$ mbar$^{-5/4}$ and $\delta p_c = 6.8$ mbar. The dashed curve is a fit of Uwaha's model using w_q from Eq. (4) with $A/\hbar = 1740$ mbar$^{7/2}\delta p^{-7/2}$ when Γ_q is set to $\Gamma_{\rm cr} = 10^{10}$ Hz.

100 mK into one single distribution which is displayed in Fig. 4.

According to standard theoretical models, nucleation is induced thermally at high temperatures and its rate $w_t(\{\delta p)\}$ is given by the usual Arrhenius law

$$w_t(\delta p) = \Gamma_t \exp\left(-\frac{E}{k_B T}\right), \tag{3}$$

where E is the energy barrier for growth of a nucleus and Γ_t is the attempt frequency. Thermal fluctuations die out at low temperatures and quantum tunneling of a virtual seed through the potential barrier remains the only physical mechanism. Its rate is given by

$$w_q(\delta p) = \Gamma_q \exp\left(-\frac{A}{\hbar}\right), \tag{4}$$

where A is two times the imaginary part of the action along the underbarrier trajectory [1,2]. The quantum attempt frequency Γ_q is different from Γ_t, but their values are not crucial for the analysis. We may approximate both by the frequency $\Gamma_{\rm cr} = k_B T/\hbar = 10^{10}$ Hz [12], which corresponds to a temperature $T_{\rm cr} \sim 100$ mK for the crossover between the quantum and thermal-activation regimes.

Uwaha [13] has shown that, in the presence of a flat wall, the arguments in the exponents of Eqs. (3) and (4) are strongly reduced at small contact angles. However, in order to explain overpressures on the order of 3 mbar, one needs an angle of $\sim$1 mrad, which seems extremely small with respect to the reported values of $\sim$2.5 rad for macroscopic crystals [14]. Another problem with Uwaha's model is that it predicts the same overpressure dependences as the bulk-nucleation model [1]: $-\ln w_q \propto A \propto 1/\delta p^{7/2}$ and $-\ln w_t \propto E \propto 1/\delta p^2$. At least our measured rates below 100 mK do not follow the form of Eq. (4) for quantum nucleation (see Fig. 4). One can reconcile Uwaha's model with our data only assuming an extremely low attempt frequency $\Gamma_q \approx 4 \times 10^3$ Hz, which looks incredibly small in light of current theories [2,8].

Another possibility is tunneling from a macroscopic seed located in a cavity on the wall. The total energy of a seed on the wall is given by

$$E = \sigma(S - S_c \cos\alpha) - V\delta\tilde{p}\,, \tag{5}$$

where α is the contact angle between the wall and the solid, V is the volume of the seed, S is the area of the solid-liquid interface, S_c is the area between the solid and the wall, and the pressure difference between the solid and liquid phases, denoted by $\delta\tilde{p}$, is connected with the measured overpressure by the relation $\delta\tilde{p} = [(\rho_s - \rho_l)/\rho_l]\delta p = (\Delta\rho/\rho_l)\delta p$ where ρ_s and ρ_l are the densities of solid and liquid, respectively. The variation of energy with respect to the seed volume yields the Laplace equation. In the case of an axisymmetric seed, there is only one curvature radius R:

$$\frac{dE}{dV} = \frac{2\sigma}{R} - \delta\tilde{p}\,. \tag{6}$$

Solid at $\delta\tilde{p} < 0$ may be stabilized by the combined action of the contact angle and the wall geometry, which together facilitate the solid/liquid interface to have a negative curvature $1/R$. This means that a small seed may survive melting and become a nucleus for the following crystal growth. Thus its role is similar to remnant vortices which sometimes play a role in vortex nucleation [15].

The growth of a remnant seed is resisted by a barrier governed by the surface geometry. The barrier disappears at some critical overpressure $\delta\tilde{p}_c$, which corresponds to an instability point where $dE/dV = d^2E/dV^2 = 0$. Assuming a smooth, analytical energy dependence near the instability point, one can then use a Taylor expansion for the energy as a function of the seed volume V:

$$E = E_0 + \delta P(V - V_0) - \frac{\lambda}{6}(V - V_0)^3. \tag{7}$$

Here V_0 is the seed volume, $\delta P = \delta\tilde{p}_c - \delta\tilde{p}$, and $\lambda = -d^3E/dV^3$. In fact, Eq. (7) is the simplest analytical form for the energy near an instability point and, therefore, it is of rather general character.

Even without specifying any values of the parameters $\delta\tilde{p}_c$ and λ, one is able to make some conclusions on the dependence of the nucleation rate on overpressure. The energy in Eq. (7) has a minimum at $V = V_0 - x_0$ and a maximum at $V = V_0 + x_0$, where $x_0 = \sqrt{2\delta P/\lambda}$. The height of the potential barrier is thus $E_b = E(V + x_0) - E(V - x_0) = \frac{4\sqrt{2}}{3}\sqrt{\delta P^3/\lambda}$, which yields for the tunneling rate

$$w_t = \Gamma_{\rm cr} \exp[-B_t(\delta p_c - \delta p)^{3/2}], \tag{8}$$

where $B_t = 4\sqrt{2}(\Delta\rho/\rho_l)^{3/2}/3\sqrt{\lambda}k_B T$. A fit of this formula to the experimental data at 500 mK is illustrated in Fig. 2.

In order to find the quantum nucleation rate, one must construct the Lagrangian for the seed:

$$L(x,\dot{x}) = \frac{1}{2} M\dot{x}^2 - \sqrt{\frac{\lambda\delta P}{2}}\, x^2 + \frac{\lambda}{6} x^3. \qquad (9)$$

Here the coordinate $x = V - V_0 + x_0$ is measured from the volume of the seed with minimum energy and the mass M is connected to the kinetic flow energy of the expanding interface. This Lagrangian with the quadratic + cubic potential energy was considered by Caldeira and Leggett [2]. Using their analysis, we obtain for the rate of MQT

$$w_q = \Gamma_{\rm cr} \exp[-B_q(\delta p_c - \delta p)^{5/4}], \qquad (10)$$

where $B_q = \frac{48}{5}(\Delta\rho/\rho_l)^{5/4}\sqrt{\sqrt{2}M}/\hbar\lambda^{3/4}$. This formula agrees well with our data below 100 mK as illustrated in Fig. 4. For the critical pressure our fit yields $\delta p_c = 6.8$ mbar. This confirms that nucleation takes place not very far from the instability point, and hence the use of a simple quadratic + cubic potential in our analysis is justified. Dissipation, which usually affects the macroscopic quantum tunneling [2,8], is not important in our case because of very high mobility K of the crystal-liquid interface at low temperatures. The parameter, which determines the effect of dissipation on quantum tunneling [2], is less than $\rho_s^{3/2}/(\Delta\rho K\delta\tilde{p}^{1/2}) \approx 5 \times 10^{-4}$, using $K \approx 400$ s/cm [16].

We tried to find an axisymmetric seed-in-a-cavity geometry which may provide the values of B_q and B_t obtained by fitting of Eqs. (8) and (10) to the experimental data. A requirement to the geometry is that the ratio between the size of the seed and its radius of curvature is on the order 10^{-3}. As also pointed out by Tsymbalenko [9], this may be a result of matching between the slope of the walls and the contact angle. We note that our geometry assumes that the contact angle is smaller than $\pi/2$, but does not require the contact angle to be very small. This is, however, only a simple example of how the seed-in-a-cavity geometry may provide an instability at small overpressures. More complicated nonaxisymmetric geometries are possible as well.

We have carefully investigated possible experimental origins for the large width of the distributions. Acoustic noise cannot be responsible for the width, since pressure changes induced by mechanical vibrations were less than 1 μbar. One possible reason is the truncation error which can be estimated to be evenly distributed between zero and $\bar{c}\Delta t \sim 0.1$ mbar where $\Delta t = 0.5$ s is the interval between the measured points of pressure. However, deconvolution of the data with this distribution does not lead to any appreciable changes in the widths of the distributions. Another possible source of statistics, which we cannot completely rule out, is a random variation among different sites of crystallization with distinct instability thresholds. A broad spectrum of instabilities seems, however, unlikely to us since the crystal is known to be generated in a well defined place with a fixed crystalline orientation.

In conclusion, we have presented experimental evidence that creation of ^{4}He crystals takes place via macroscopic quantum tunneling at $T < 100$ mK. We have suggested a model which relates the nucleation process to an instability of the crystal seed preexisting in some cavity on the wall. The model is in a good agreement with the observed overpressure dependence of the nucleation rate.

We want to thank S. Balibar, Y. Kondo, J. Kurkijärvi, O. Lounasmaa, M. Paalanen, A. Parshin, E. Polturak, V. Tsymbalenko, and G. Volovik for useful comments and critical remarks. This work was supported by the Academy of Finland and by the Human Capital and Mobility Program ULTI of the European Community.

*Permanent address: Ioffe-Physico Technical Institute, St. Petersburg 194021, Russia.

[1] I. M. Lifshitz and Yu. Kagan, Zh. Eksp. Teor. Fiz. **62**, 385 (1972) [Sov. Phys. JETP **35**, 206 (1972)].
[2] A. O. Caldeira and A. J. Leggett, Ann. Phys. (N.Y.) **149**, 374 (1983).
[3] J. C. Davis, J. Steinhauer, K. Schwab, Yu. M. Mukharsky, A. Amar, Y. Sasaki, and R. E. Packard, Phys. Rev. Lett. **69**, 323 (1992).
[4] G. G. Ihas, O. Avenel, R. Aarts, R. Salmelin, and E. Varoquaux, Phys. Rev. Lett. **69**, 327 (1992).
[5] T. Satoh, M. Morishita, M. Ogata, and S. Katoh, Phys. Rev. Lett. **69**, 335 (1992).
[6] S. Balibar, C. Guthmann, H. Lambare, P. Roche, E. Rolley, and H. J. Maris, J. Low Temp. Phys. **101**, 271 (1995).
[7] G. Blatter, M. V. Feigel'man, V. B. Geshkenbein, A. I. Larkin, and V. M. Vinokur, Rev. Mod. Phys. **66**, 1125 (1994).
[8] J. M. Martinis, M. H. Devoret, and J. Clarke, Phys. Rev. B **35**, 4682 (1987).
[9] V.L. Tsymbalenko, J. Low Temp. Phys. **88**, 55 (1992).
[10] A. V. Babkin, H. Alles, P. J. Hakonen, A. Ya. Parshin, J. P. Ruutu, and J. P. Saramäki, Phys. Rev. Lett. **75**, 3324 (1995); J. P. Ruutu, P. J. Hakonen, A. V. Babkin, A. Ya. Parshin, J. S. Penttilä, J. P. Saramäki, and G. Tvalashvili, Phys. Rev. Lett. **76**, 4187 (1996).
[11] S. Balibar, B. Castaing, and C. Laroche, J. Phys. (Paris) Lett. **41**, 283 (1980).
[12] See, e.g., P. Hänggi, P. Talkner, and M. Borkovec, Rev. Mod. Phys. **62**, 251 (1990).
[13] M. Uwaha, J. Low Temp. Phys. **52**, 15 (1983).
[14] J. Landau, S. G. Lipson, L. M. Määttänen, L. S. Balfour, and D. O. Edwards, Phys. Rev. Lett. **45**, 31 (1980).
[15] R. J. Donnelly, *Quantized Vortices in Helium II* (Cambridge University Press, New York, 1991).
[16] E. Rolley, C. Guthmann, E. Chevalier, and S. Balibar, J. Low Temp. Phys. **99**, 851 (1995).